

VNU Journal of Science: Mathematics - Physics





Original Article

Indentation Response of the Auxetic Bone-inspired Cellular Structure Materials

Nguyen Van Luan^{1,2}, Pham Dinh Nguyen², Ngo Dinh Dat², Vu Minh Anh², Nguyen Dinh Duc², Nguyen Van Thuong^{2,*}

¹Thai Nguyen University of Technology, Thai Nguyen, Vietnam ²VNU University of Engineering and Technology, 144 Xuan Thuy, Cau Giay, Hanoi, Vietnam

> Received 9th February 2025 Revised 05th March 2025; Accepted 16th June 2025

Abstract: in this work we investigate the indentation response of the auxetic cellular structure materials. The auxetic cellular structure material is selected as the newly bone-inspired cellular structure material. The elastic material properties of this material are characterized by nine elastic constants. Thus, to study the indentation responses of the auxetic bone-inspired cellular structure materials, the solutions for the indentation of a rigid indenter on an anisotropic elastic half-plane are employed. It was found that auxetic (with a negative Poisson ratio) bone-inspired cellular structure materials can effectively reduce the local contact pressure under the indenter compared to those with positive and zero Poisson ratios. The auxetic BCS material, therefore, has great potential in protecting key engineering structures.

Keywords: auxetic, indentation, bone-inspired, cellular structure material.

1. Introduction

In recent years, material science and engineering have witnessed significant advancements in the design and application of cellular materials. These materials possess several advantages, such as lightweight, excellent energy absorption, and impact resistance, which lead to their widespread use in various engineering applications [1-4]. Among different cellular structure materials, bone-inspired materials have shown great potential in mitigating the influences of extreme loadings and have recently attracted the attention of many researchers [5-9]. Indentation response is a critical parameter in evaluating the durability and robustness of materials. It can refer to the ability to withstand localized

E-mail address: thuong.nv@vnu.edu.vn

^{*} Corresponding author.

deformation and stress when subjected to an indenting force. This property is vital across a wide range of applications, from protective and impact-resistant components to structural supports and medical implants [10, 11]. Introducing auxetic bone-inspired cellular structures (ABCS) into these domains promises superior performance. To the best of the author's knowledge, no published work has investigated the indentation response of bone-inspired cellular materials (BCS) in the literature. This paper explores the indentation responses of the ABCS structure, focusing on their contact behavior under the indenting force and comparing their performance with positive and zero Poisson ratio BCS materials. Understanding the contact behaviors of the ABCS provides valuable insights into indentation response, which could pave the way for innovative material solutions with enhanced resilience and functionality.

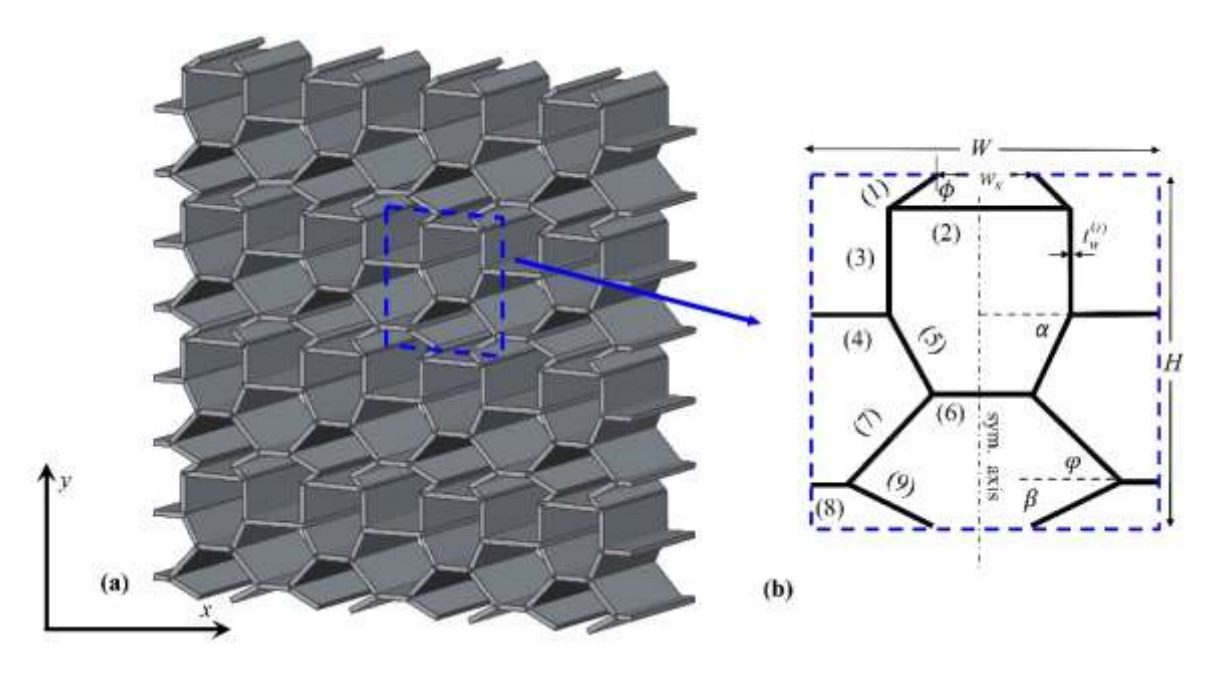


Figure 1. (a) Bone-inspired cellular structure material and (b) its geometric parameters [9].

2. A brief on Bone-inspired Cellular Structure Materials

The BCS material was first introduced in the published paper [7, 8] based on the hybrid design of cancellous bone. The BCS model consists of two different sub-cells with nine-cell walls whose geometric parameters are depicted in Fig. 1. In this figure, l_i and $t_i^{(w)}$, i=1,2,...,9 are, respectively, the length and the cell wall's thicknesses. If we let β and α be, respectively, the upper and lower sub-cell angles, H and H0 be, respectively, the height and width of the unit cell, and H1 and H2 be, respectively, the upper and lower tie lengths, the length of the cell walls can be evaluated as [9]

$$l_{1} = \sqrt{e^{2} + (H/8)^{2}}, \ l_{2} = l_{u}/2, \ l_{3} = H/4,$$

$$l_{4} = (W - l_{b} - 2c)/2, \ l_{5} = H/(4\sin\alpha), \ l_{6} = l_{b}/2,$$

$$l_{7} = \sqrt{d^{2} + (H/4)^{2}}, \ l_{8} = (W - b)/2, l_{9} = H/(8\sin\beta),$$
(1)

and

$$a=H/(8\tan\beta), \ e=H/(8\tan\phi), \ b=w_s+H/(4\tan\beta),$$

$$c=H/(4\tan\alpha), \ d=(b-l_b)/2, \ w_s=l_u-2e,$$

$$\varphi=\tan^{-1}(H/4d), \ l_u-l_b-2c=0.$$
(2)

Using Castigliano's theorem and the mechanisms of shear strain/stress deformation in the analysis, it was found that BCS materials can be homogenized and represented through 9 independent elastic constants depending on the angle β [9]. The Poisson ratios, therefore, can vary from positive to negative [9]. When the Poisson ratio is negative, the materials are called auxetic BCS materials. If PLA is considered the base material of BCS cells for three different horizontal cell wall thicknesses, the material properties of BCS materials are listed below. In this table, Case 1 has a uniform thickness of 1 mm, Case 2 has double horizontal cell walls of 2 mm and 1 mm for other cell walls, and Case 3 has a triple horizontal cell wall and 1 mm for other cell walls. The subscripts 1, 2, and 3 denote the x, y and z directions, respectively.

	β	E_1	E_2	E_3	G_{31}	G_{32}	G_{12}	v_{13}	v_{23}	v_{12}
Case 1	55	21.02	59.48	680.5	142.14	109.89	0.34	0.011	0.031	0.13
	82.5	21.51	83.04	692.12	142.73	113.62	0.24	0.011	0.042	0
	130	20.06	52.09	753.8	172.13	107.06	0.13	0.009	0.024	-0.19
Case 2	55	22.06	60.01	987.57	255.88	109.89	0.56	0.008	0.021	0.13
	82.5	22.71	84.56	1022.63	265.14	113.62	0.47	0.008	0.029	0
	130	21.24	57.67	1124.38	309.38	107.06	0.31	0.007	0.018	-0.21
Case 3	55	22.43	60.22	1294.65	369.61	109.89	0.6	0.006	0.016	0.13
	82.5	23.15	85.42	1353.14	387.55	113.62	0.52	0.006	0.022	0
	130	21.67	69.91	1494.95	446.63	107.05	0.36	0.005	0.016	-0.22

Table 1. Equivalent elastic constants of BCS materials for three different cases [9]. Here, the unit of the elastic and shear moduli is MPa

With the above equivalent elastic constants, we employ the solutions of the indentation of a rigid indenter on an anisotropic elastic half-plane to investigate the indentation response of BCS materials.

3. Indentation of BCS Materials

Consider a frictional contact of a parabolic indenter on an elastic foundation made of the BCS material (see Fig. 2). The main focus of the problem is to determine the contact stress, contact region, and surface deformation. For the present problem, the contact region, contact stress, and surface deformation can be described by the following set of equations, written in the Cartesian coordinate (x,y,z) [12-14]

$$\sigma_{ij} = C_{ijkl} \varepsilon_{kl}, \ \varepsilon_{ij} = \frac{1}{2} (u_{i,j} + u_{j,i}), \ \sigma_{ij,j} = 0, \ i, j, k, l = 1, 2, 3,$$
 (3)

$$t_1(x) = \pm \kappa t_2(x), \ u_2(x) = u_0 + f(x), \ t_3(x) = 0, \ x \in (-a,b),$$
 (4)

$$t_i(x) = 0, i = 1, 2, 3, x \notin (-a, b),$$
 (5)

$$\int_{-a}^{b} t_2(x)x dx = P,\tag{6}$$

where P is the applied load in direction y; $f(x) = x^2 / 2R$ is the profile of the parabolic indenter, where R is the radius of the curvature; -a and b denote two ends of the contact region, $a \le w, b \le w$ where w is the width of the indenter; u_i and $t_i, i = 1, 2, 3$ are the displacements and tractions in the x, y, and z directions. ε_{ij} and σ_{ij} , i, j = 1, 2, 3, are strains and stresses. The traction and stresses are related by $t_i = \sigma_{ij} n_j$, i, j = 1, 2, 3, where n_j denotes the unit normal vector of the contact surface; C_{ijkl} is the elastic stiffness tensor obtained from Table 1 using the relation (1.43) or (1.46) in [15] and κ is the friction coefficient of the contact surface, and its sign depends on the loading direction [12-14].

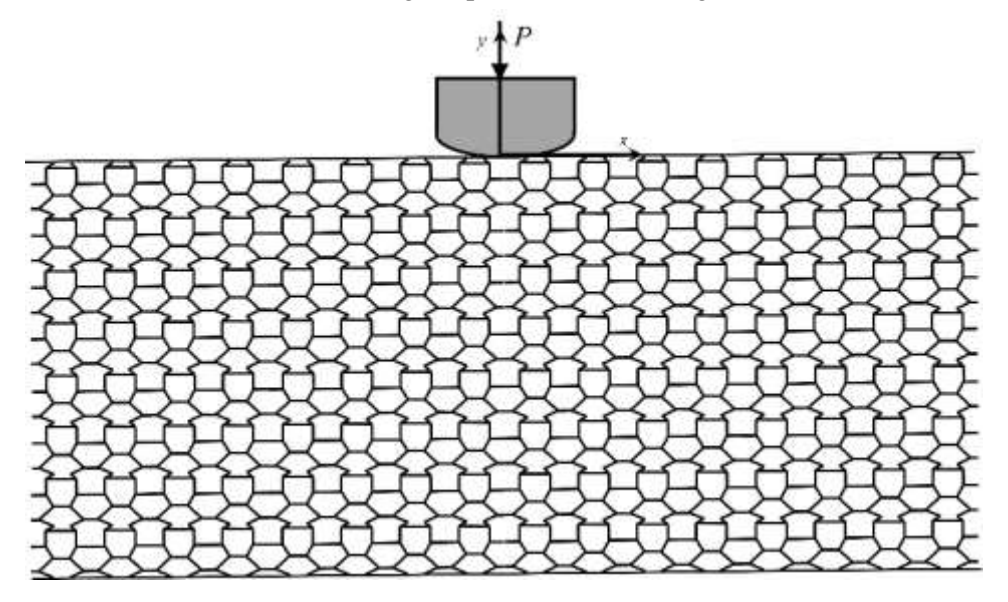


Figure 2. Frictional indentation of a parabolic indenter on a BCS foundation.

The literature provides several ways to solve the above equations [15-17]. Among these methods, the Stroh complex variable formalism and the analytical continuation method are interesting to many researchers due to their mathematical elegance and ability to solve complex problems with anisotropic/orthotropic elastic materials. Using the Stroh complex variable formalism and the analytical continuation method, the solutions to the problem can be formulated as a Hilbert problem, and its solutions can be presented as follows [15].

$$\mathbf{u} = 2\operatorname{Re}\left\{\mathbf{Af}(p)\right\}, \quad \phi = 2\operatorname{Re}\left\{\mathbf{Bf}(p)\right\},\tag{7}$$

$$\mathbf{f}(p) = \mathbf{B}^{-1}\mathbf{\theta}(p), \ \mathbf{\theta}(p) = (\theta_1(p), \ \theta_2(p), \ \theta_3(p))^T, \tag{8}$$

$$\theta_1(p) = \pm \kappa \theta_2(p), \ \theta_3(p) = 0,$$

$$\theta_2'(p) = \frac{i}{(\tau + \overline{\tau})R} \left\{ p - \chi_0(p) \left[g(p) + \frac{(\tau + \overline{\tau})RP}{2\pi} \right] \right\},\tag{9}$$

$$t_2(x) = -\frac{i\chi_0(x^{-})}{\tau R} \left\{ g(x) + \frac{(\tau + \overline{\tau})RP}{2\pi} \right\}, \ x \in [-a, b],$$
 (10)

$$u_2'(x) = -\frac{1}{R} \left\{ x - \chi_0(x^-) \left[g(x) + \frac{(\tau + \overline{\tau})RP}{2\pi} \right] \right\}, \ x \notin [-a, b],$$
 (11)

$$\chi_0(p) = (p+a)^{-\delta} (p-b)^{\delta-1}, \ \delta = \frac{1}{2} \arg(-\overline{\tau} / \tau),
\chi_0(x^-) = \lim_{x \to 0^-, \ y = 0} \chi_0(p),$$
(12)

$$g(p) = p^{2} - [b - (a+b)\delta]p + \frac{1}{2}(a+b)^{2}\delta(\delta - 1).$$
 (13)

In the above equations, $\theta_2(p)$ is the sectional holomorphic complex function and $\theta_2'(p)$ stands for its derivative w.r.t p, where $p = x + \mu_{\alpha} y$; μ_{α} is the material eigenvalue; **A** and **B** are the material eigenmatrices. As how to obtain μ_{α} , **A** and **B**, please refer to the book of Hwu [15] for detailed procedures. κ is the friction coefficient and the sign ahead of κ depends on the intended sliding direction of the indenter; $\tau = \overline{m}_{22} \pm \kappa \overline{m}_{21}$ where m_{21} and m_{22} are the {21} and {22} components of the matrix \mathbf{M}^{-1} where $\mathbf{M} = -i\mathbf{B}\mathbf{A}^{-1}$ [15]. The contact region denoted by -a and b (a > 0 and b > 0) can be obtained by setting the normal traction $t_2(x)$ in Eq. (10) equal to zero at x = -a and x = b. The resulting expressions are

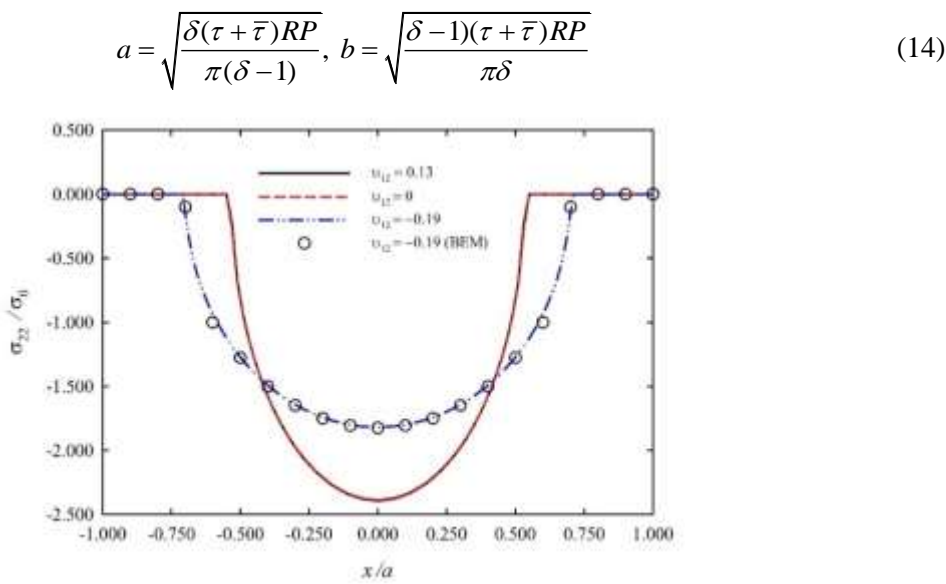


Figure 3. Contact pressure under the indenter for different types of BCS materials. Here, $\sigma_0 = -P/2a$.

4. Results and Discussion

4.1. Indentation Response of BCS Materials

This section considers the frictionless contact of a rigid indenter and an elastic foundation. The indenter width is 0.02 m, and its radius of curvature is R = 2 m. It is subjected to the load P = -100 N/m. The elastic foundation is made of BCS materials whose properties are selected as Case 1 in Table 1. Figure 3 presents the contact pressure under the indenter for the different BCS materials. We see that our analytical results are well-matched with those obtained by the boundary element method [18] for the case of the negative Poisson ratio. We also observe that the magnitude of contact pressure is smallest

when the Poisson ratio is negative. With the smaller contact pressure, the ABCS provides a better performance in protecting engineering structures than those with positive and zero Poisson ratios.

4.2. Effect of Friction

To study the effect of friction, we consider the indentation of a parabolic indenter on an auxetic BCS material, whose material properties are given as Case 1 with the Poisson ratio v = -0.19. Fig. 4 depicts the contact pressure under the indenter. It can be observed that when the friction coefficient increases, the contact region moves to the right, which is similar to the observation obtained in [12-14, 18, 19] for the other composite materials.

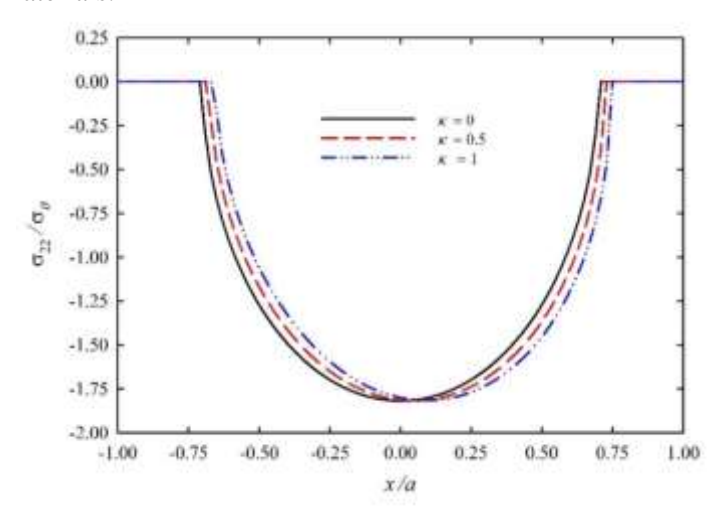


Figure 4. Contact pressure along the auxetic BCS foundation surface with different frictional coefficients.

4.3. Effect of BCS Cell Wall Thickness

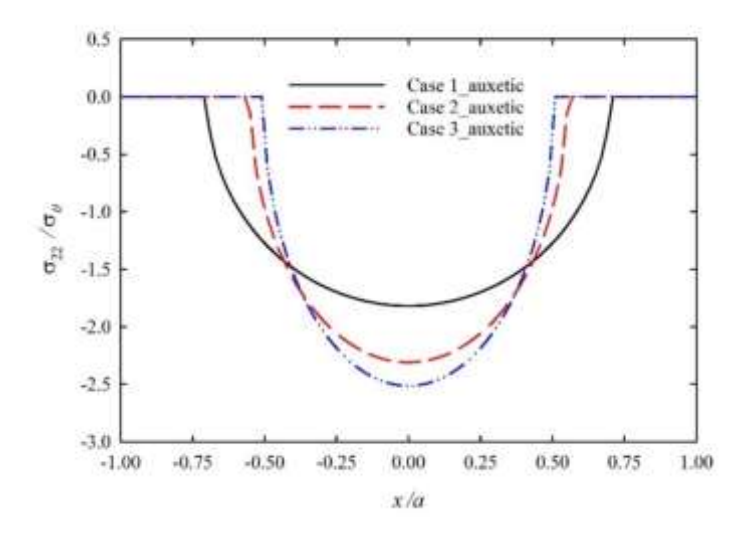


Figure 5. Influence of the horizontal cell wall thickness on the contact pressure along the contact surface of BCS materials.

To study the influence of the cell wall thickness, we consider the indentation of the ABCS materials whose cell wall thickness varies as uniform, double, and triple thicknesses mentioned in Table 1. Figs. 5 and 6 show the contact pressure under the indenter and the surface deformation along the BCS upper surface for three different cases. It can be deduced from these figures that the contact region reduces, the contact stress under the indenter increases, and the relative magnitude of the surface deformation reduces when the horizontal cell wall thickness increases, which is reasonable and consistent with our engineer's intuition. By controlling the thickness of the BCS cell wall, we can control its performance under the indentation.

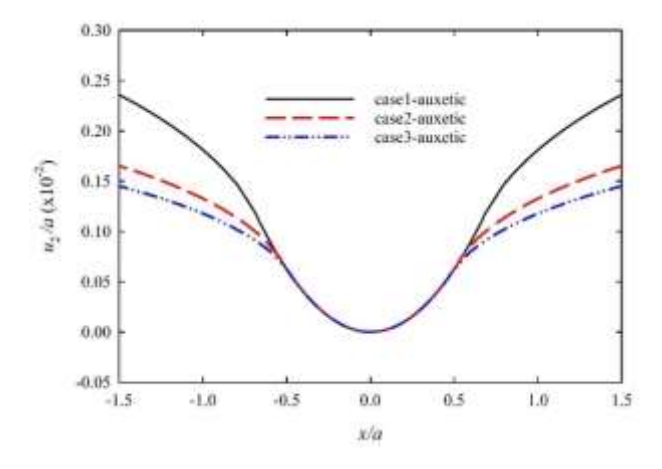


Figure 6. Influence of the horizontal cell wall thickness on the surface deformation along the contact surface of BCS.

4.4. Effect of Indenter Profile

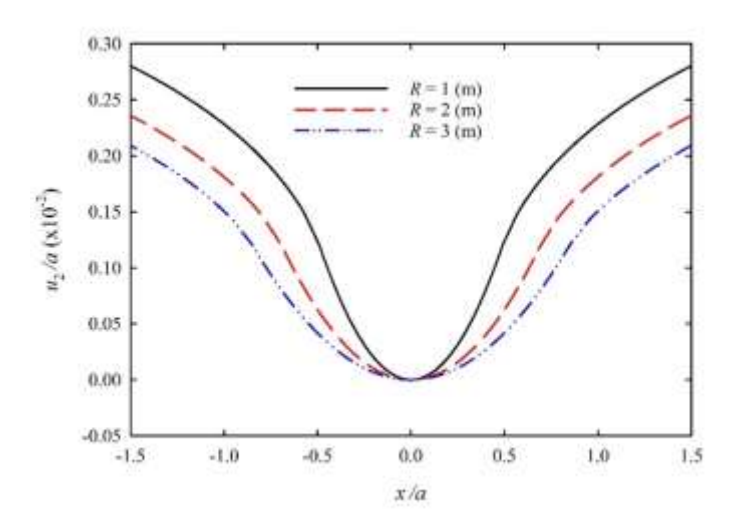


Figure 7. Influence of the indenter profile on the surface deformation along the contact surface of BCS.

In this section, the influence of the punch profile on the indentation responses of the auxetic material is investigated. The material is chosen as Case 1 with the Poisson ratio v = -0.19. The radius of the indenter is R = 1,2, and 3 m. Figs. 7 and 8 show the contact pressure and surface deformation of the

BCS foundation. From these figures, we see that the contact region increases, and the maximum contact pressure and the relative surface deformation reduce when the radius of the indenter increases. These observations are reasonable and consistent with our engineer's intuition.

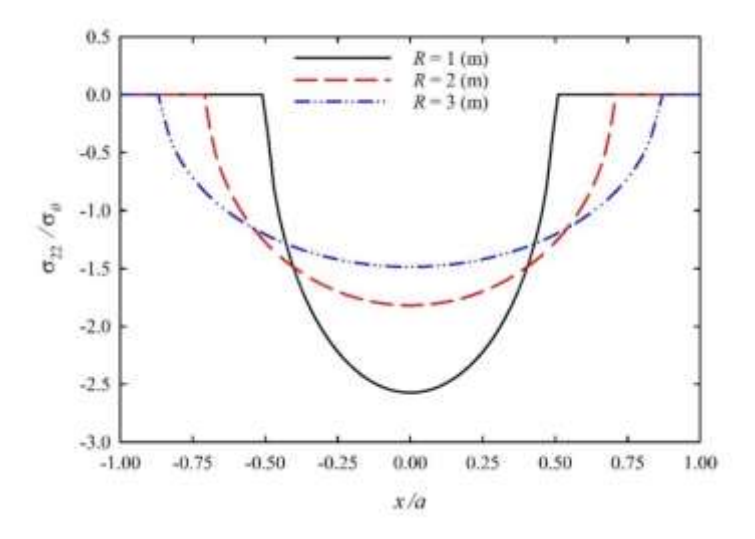


Figure 8. Influence of the indenter profile on the contact pressure along the contact surface of BCS.

5. Conclusions

We investigated the indentation response of the bone-inspired cellular structure material using the Stroh complex formalism and the analytical continuation method. We found that the auxetic BCS materials reduce the localized contact stress, providing better indentation protection than those with positive and zero Poisson ratios. The indentation response of the BCS materials can also be controlled by the cell wall thickness. Besides these findings, we also investigated the influence of friction coefficients and indenter profiles on the contact and indentation behaviors. The investigations presented in this work provide helpful information on designing and optimizing structural systems with bone-inspired cellular structure materials.

Acknowledgments

This work was supported by the Grant in Mechanics of the National Foundation for Science and Technology Development of Viet Nam – NAFOSTED code 107.02-2023.21. The authors are grateful for this support.

References

- [1] J. Banhart, Manufacture, Characterisation and Application of Cellular Metals and Metal Foams, Progress in Materials Science, Vol. 46, Iss. 6, 2001, pp. 559-632, https://doi.org/10.1016/S0079-6425(00)00002-5.
- [2] T. Wang, Z. Li, L. Wang, X. Zhang, Z. Ma, In-plane Elasticity of a Novel Arcwall-based Double-arrowed Auxetic Honeycomb Design: Energy-based Theoretical Analysis and Simulation, Aerospace Science and Technology, Vol. 127, 2022, pp. 107715, https://doi.org/10.1016/j.ast.2022.107715.

- [3] A. Y. N. Sofla, S. A. Meguid, K. T. Tan, W. K. Yeo, Shape Morphing of Aircraft Wing: Status and Challenges, Materials & Design, Vol. 31, Iss. 3, 2010, pp. 1284-1292, https://doi.org/10.1016/j.matdes.2009.09.011.
- [4] A. Ghazlan, T. Ngo, T.S. Le, T. V. Le, Automated Simulation Techniques for Uncovering High-performance Bioinspired Cellular Structures under Blast Loads, Journal of Sandwich Structures & Materials, Vol. 24, Iss. 1, 2022, pp. 517-535, https://doi.org/10.1177/10996362211020458.
- [5] F. Ghorbani, H. Gharehbaghi, A. Farrokhabadi, A. Bolouri, Investigation of the Equivalent Mechanical Properties of the Bone-inspired Composite Cellular Structure: Analytical, Numerical and Experimental Approaches, Composite Structures, Vol. 309, 2023, pp. 116720, https://doi.org/10.1016/j.compstruct.2023.116720.
- [6] F. Ghorbani, H. Gharehbaghi, A. Farrokhabadi, A. Bolouri, Evaluation of the Mechanical Properties and Energy Absorption in a Novel Hybrid Cellular Structure, Aerospace Science and Technology, Vol. 148, 2024, pp. 109105, https://doi.org/10.1016/j.ast.2024.109105.
- [7] A. Ghazlan, T. Ngo, T. Nguyen, S. Linforth, T. V. Le, Uncovering a High-performance Bio-mimetic Cellular Structure from Trabecular Bone, Scientific Reports, Vol. 10, 2020, pp. 14247, https://doi.org/10.1038/s41598-020-70536-7.
- [8] A. Ghazlan, T. Nguyen, T. Ngo, S. Linforth, T. V. Le, Performance of a 3D Printed Cellular Structure Inspired by Bone. Thin-Walled Structures, Vol. 151, 2020, pp. 106713, https://doi.org/10.1016/j.tws.2020.106713.
- [9] V. T. Nguyen, N. D. Khoa, T. Ngo, N. D. Duc, Analytical Investigation of In-plane and Out-of-plane Elastic Properties of Bone-inspired Cellular Structures, Aerospace Science and Technology, Vol. 147, 2024, pp. 109012, https://doi.org/10.1016/j.ast.2024.109012.
- [10] D. Photiou, N. Prastiti, E. Sarris, G. Constantinides, On the Conical Indentation Response of Elastic Auxetic Materials: Effects of Poisson's Ratio, Contact Friction and Cone Angle, International Journal of Solids and Structures, Vol. 81, 2016, pp. 33-42, https://doi.org/10.1016/j.ijsolstr.2015.10.020.
- [11] I. I. Argatov, R. G. Díaz, F. J. Sabina, On Local Indentation and Impact Compliance of Isotropic Auxetic Materials from the Continuum Mechanics Viewpoint, International Journal of Engineering Science, Vol. 54, 2012, pp. 42-57, https://doi.org/10.1016/j.ijengsci.2012.01.010.
- [12] V. T. Nguyen, G. T. Chen, C. Hwu, Multibody Contact of Two-dimensional Anisotropic Elastic/Piezoelectric/Magneto-Electro-Elastic Solids, Engineering Analysis with Boundary Elements, Vol. 146, 2023, pp. 767-785, https://doi.org/10.1016/j.enganabound.2022.11.019.
- [13] V. T. Nguyen, C. Hwu, Boundary Element Method for Contact between Multiple Rigid Punches and Anisotropic Viscoelastic Foundation, Engineering Analysis with Boundary Elements, Vol. 118, 2020, pp. 295-305, https://doi.org/10.1016/j.enganabound.2020.07.001.
- [14] V. T. Nguyen, C. Hwu, A Unified Fullfield Solution for Indentation of an Anisotropic Piezoelectric Half-plane by Multiple Rigid Punches, Mechanics of Advanced Materials and Structures, Vol. 30, Iss. 19, 2023, pp. 3897-3911, https://doi.org/10.1080/15376494.2022.2084802.
- [15] C. Hwu, Anisotropic Elastic Plates, New York, Springer, 2010.
- [16] N. I. Muskhelishvili, Some Basic Problems of the Mathematical Theory of Elasticity, Springer, Dordrecht, 1977.
- [17] K. L. Johnson, Contact Mechanics, Cambridge University Press, 2012.
- [18] V. T. Nguyen, C. Hwu, Indentation by Multiple Rigid Punches on Two-dimensional Anisotropic Elastic or Viscoelastic Solids, International Journal of Mechanical Sciences, Vol. 178, 2020, pp. 105595, https://doi.org/10.1016/j.ijmecsci.2020.105595.
- [19] V. T. Nguyen, Q. T. Bui, A Semi-Analytical Approach for Two-dimensional Frictional Contact of Anisotropic Magneto-Electro-Elastic Solids, International Journal of Solids and Structures, Vol. 286-287, 2024, pp. 112565, https://doi.org/10.1016/j.ijsolstr.2023.112565.